JACS
JOURNAL OF THE AMERICAN CHEMICAL SOCIETY

pubs.acs.org/JACS

Communication

Scale-Up of Room-Temperature Constructive Quantum Interference from Single Molecules to Self-Assembled Molecular-Electronic Films

Xintai Wang,[#] Troy L. R. Bennett,[#] Ali Ismael,[#] Luke A. Wilkinson, Joseph Hamill, Andrew J. P. White, Iain M. Grace, Oleg V. Kolosov, Tim Albrecht, Benjamin J. Robinson,[*] Nicholas J. Long,[*] Lesley F. Cohen,[*] and Colin J. Lambert[*]

Cite This: *J. Am. Chem. Soc.* 2020, 142, 8555−8560

Read Online

ACCESS | Metrics & More | Article Recommendations | Supporting Information

ABSTRACT: The realization of self-assembled molecular-electronic films, whose room-temperature transport properties are controlled by quantum interference (QI), is an essential step in the scale-up of QI effects from single molecules to parallel arrays of molecules. Recently, the effect of *destructive* QI (DQI) on the electrical conductance of self-assembled monolayers (SAMs) has been investigated. Here, through a combined experimental and theoretical investigation, we demonstrate chemical control of different forms of *constructive* QI (CQI) in cross-plane transport through SAMs and assess its influence on cross-plane thermoelectricity in SAMs. It is known that the electrical conductance of single molecules can be controlled in a deterministic manner, by chemically varying their connectivity to external electrodes. Here, by employing synthetic methodologies to vary the connectivity of terminal anchor groups around aromatic anthracene cores, and by forming SAMs of the resulting molecules, we clearly demonstrate that this signature of CQI can be translated into SAM-on-gold molecular films. We show that the conductance of vertical molecular junctions formed from anthracene-based molecules with two different connectivities differ by a factor of approximately 16, in agreement with theoretical predictions for their conductance ratio based on CQI effects within the core. We also demonstrate that for molecules with thioether anchor groups, the Seebeck coefficient of such films is connectivity dependent and with an appropriate choice of connectivity can be boosted by ∼50%. This demonstration of QI and its influence on thermoelectricity in SAMs represents a critical step toward functional ultra-thin-film devices for future thermoelectric and molecular-scale electronics applications.

Molecular electronic devices have the potential to deliver logic gates, sensors, memories, and thermoelectric energy harvesters with ultra-low power requirements and sub-10-nm device footprints.[1−4] Single-molecule electronic junctions[5−12] and self-assembled monolayers (SAMs)[13−15] have been investigated intensively over the past few years, because their room-temperature electrical conductance has been shown to be controlled by destructive quantum interference (DQI).[16−20] More recently the effect of quantum interference (QI) on the Seebeck coefficient of single molecules has also been studied.[21−26] Figure 1A illustrates an example where a room-temperature constructive quantum interference (CQI) effect would be expected from an anthracene molecular core. Here, electrical current is injected into and collected from the core via the green arrows, or alternatively via the red arrows.

Such a change in connectivity in a classical resistor network would lead to only a small change in electrical conductance. In contrast, theory predicts and experiment confirms[27−29] that the room temperature, single-molecule, low-bias electrical conductance G_1 for the green connectivity is approximately an order of magnitude greater than the conductance G_2 of the red connectivity. This is a clear signature of room-temperature phase-coherent transport and of the varying degrees of CQI for the two different connectivities. The chemical realization of the green connectivity is molecule **1** in Figure 1, in which the terminal groups attached to electrodes inject a current into the

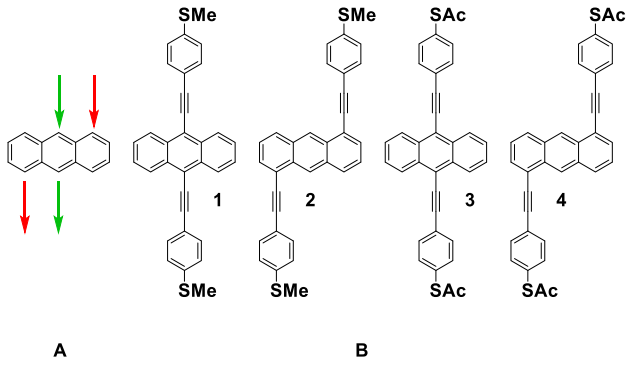

Figure 1. Structures of studied molecules. (A) Sketch of an anthracene core with connectivities 7,2′ and 1,5′. (B) Chemical realizations of molecular wires with anthracene cores. Molecules **1** and **3** correspond to the 7,2′ connectivity, while **2** and **4** correspond to the 1,5′ connectivity.

Received: January 20, 2020
Published: April 28, 2020

anthracene core via alkyne linkages. Similarly, molecule **2** is a realization of the red connectivity. **3** and **4** are alternative realizations of the red and green connectivities, in which the thioether terminal groups are replaced by thioacetate groups (which can be deprotected *in situ* to grant terminal thiols for gold binding). These terminal anchor groups were chosen to demonstrate that further control over interfacial coupling and energy level alignment between molecules and electrodes could be achieved.[30,31] Our aim is to create SAMs from these compounds, demonstrate that these single-molecule signatures of CQI can be translated into SAM-based devices, and assess the effect of CQI on their Seebeck coefficients. We indeed find that the electrical conductances of SAMs formed from **1** and **3** are significantly higher than those of SAMs formed from **2** and **4**. We also measure and calculate the Seebeck coefficients of these SAMs and show that the sign and magnitude of their thermopower is determined by a combination of their connectivities and the nature of their (thiolate or thioether) anchor groups. It should be noted that while thiol groups generally lead to stronger binding and superior film stability than thioethers,[32] the latter are preferential, where intermolecular interactions within the SAM may result in monolayer reorganization during assembly.[33,34]

Our choice of connectivities in Figure 1 was guided by "magic ratio theory",[27] which predicts that the ratio G_1/G_2 of the low-bias, single-molecule conductances of **1** and **2** (**3** and **4**) should be $G_1/G_2 = 16$ (SI, Figure S28). This simple theory illustrates how connectivity alone contributes to conductance ratios, without including chemical effects or Coulomb interactions. When the latter are included, recent studies[35] indicate that the qualitative trend in the ratio is preserved (i.e., that $G_1/G_2 \gg 1$), but the precise value should be calculated using *ab initio* methods. Our aim is to determine if this single-molecule signature of QI is preserved or modified in a SAM, where intermolecular interactions are also expected to play a role.

Figure 2 shows the frontier orbitals of **1** and **2** and, in agreement with magic ratio theory, confirms the presence of

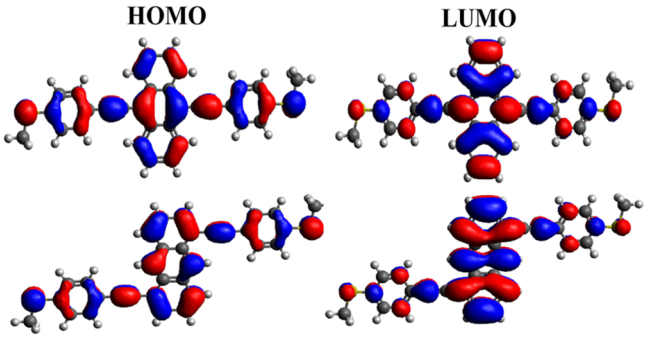

Figure 2. Frontier orbitals for **1** and **2**: HOMO and LUMO orbitals for molecule **1** (top) and molecule **2** (bottom). (Orbitals for **3** and **4** are shown in the SI.) Red (blue) corresponds to regions in space of positive (negative) orbital amplitude.

CQI, which occurs when the HOMO has different colors (representing different amplitudes) at the ends of the molecule (i.e., blue at one end and red at the other) and the LUMO has the same color (i.e., red at both ends).[29,36−38]

Molecules **1** and **2** bearing thioether termini could be synthesized from bromoanthracenes through the use of standard Sonagashira chemistry (see Scheme 1, top); however,

Scheme 1. Synthesis of Studied Molecules: Representative Synthetic Pathway Illustrating the Construction of Symmetric Anthracenes through the Use of Sonagashira (Top) and *Trans*-protection (Bottom) Reactions

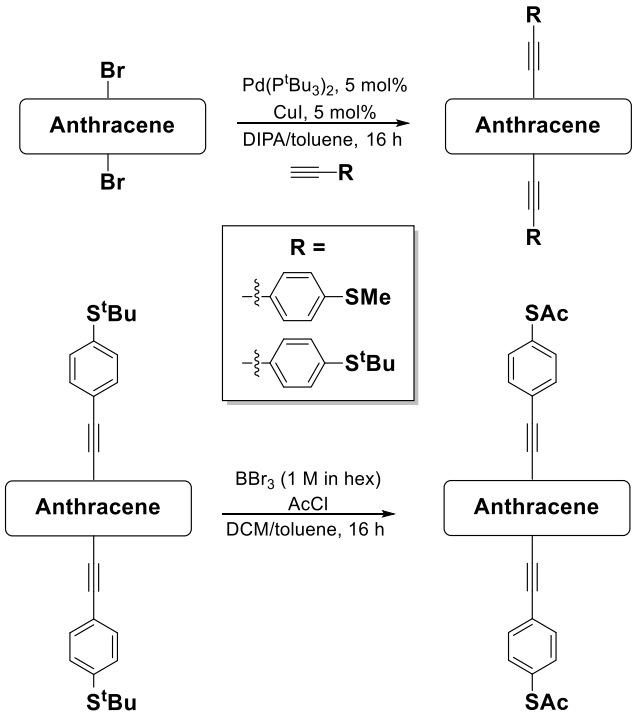

this same strategy could not be used to synthesize the thioacetate derivatives (**3** and **4**). This is due to a competing cyclo-oligomerization reaction that occurs when reacting a thioacetate-terminated phenylacetylide moiety in the presence of a palladium catalyst.[39] As a result of this, a *trans*-protection strategy was employed utilizing a *tert*-butyl-protected thiol (see Scheme 1, bottom). Initially, dibromoanthracenes were reacted with the alkyne of choice (either 4-ethynyl-*tert*-butylthioether or 4-ethynylthioanisole) to generate symmetrically disubstituted products (**1**, **2**, **3A**, and **4A**). All compounds could be purified via flash column chromatography and were obtained in good yields (>60%). Thioacetate-substituted anthracenes (**3** and **4**) were then obtained through *trans*-protection reactions of **3A** and **4A**, respectively. Molecule **4** could be purified through the use of flash chromatography alone, however recrystallization was required to isolate molecule **3**, resulting in a slightly reduced yield (see SI section 1.3).

Deposited molecular films were characterized by atomic force microscopy (AFM), nanoscratching,[40−42] and polished Au-coated quartz crystal microbalance (QCM), which suggested the formation of high-uniformity SAMs with thicknesses in the range of 1.1−1.4 nm (SI Table S5); corresponding to a monolayer of molecules in a perpendicular configuration with a tilt angle of 30°−50°.[43,44] All molecular films were grown on freshly prepared template stripped Au substrates[45,46] with a surface roughness of 80−150 pm (see Methods in the SI). Molecular conductance was characterized by conductive AFM (cAFM), where the number of molecules under the probe is estimated from the contact area between probe and sample surface (obtained via Hertz model[47−49]) and the single-molecule occupation area obtained from QCM and AFM.

https://dx.doi.org/10.1021/jacs.9b13578
J. Am. Chem. Soc. 2020, 142, 8555−8560

Aggregate conductance vs voltage histograms at low bias (−0.3 to 0.3 V) for molecules **1**−**4** are shown in Figure 3a,c,

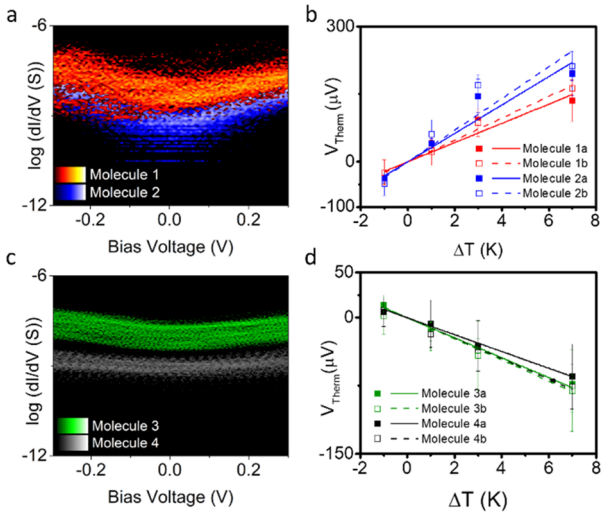

Figure 3. Electrical and thermoelectrical properties of SAMs. (a, c) Aggregate conductance vs voltage histogram of molecular conductance (molecules **1**, **2** (a), and **3**, **4** (c)), with bias voltage between −0.3 and −0.3 V. (b, d) Linear fit plot of thermal voltage vs ΔT ($T_{sample} - T_{probe}$) for molecules **1**, **2** (b) and **3**, **4** (d). SAMs Xa and SAMs Xb indicate two measured samples.

while Figure 3b,d shows the linear fit of thermal voltage vs ΔT for different junction systems (see SI Figure S36 for detailed comparison of molecules **1** and **2**). The slope of the fit, $V_{thermal}/\Delta T$, related with the Seebeck coefficient of the junction via the equation: $S_{junction} - S_{probe\text{-}Au} - V_{thermal}/\Delta T$ (the detailed number listed in Table 1). The Seebeck measurements of all SAMs were operated on two separate samples prepared with the same method (labeled as SAMs Xa and SAMs Xb), and similar Seebeck coefficient values were obtained, which confirmed the reliability of the measurement (Figure S37). The opposite slope of linear fit for $V_{thermal}/\Delta T$ between **1**,**2** and **3**,**4** demonstrates that the exchange of anchor groups leads to a change in sign for Seebeck coefficient.

From the statistics of >200 different I−V curves measured at different locations, the statistically most-probable zero-bias differential conductance for molecule **1** is 10.2 times larger than that for molecule **2**, and 14.2 times larger than that of molecule **3**.

To compute the electrical conductance of molecules **1**−**4**, we use density functional theory combined with the quantum transport code Gollum[50] to obtain the transmission coefficient describing electrons of energy E passing from the source to the drain electrodes, from which the room-temperature electrical conductance and Seebeck coefficient are determined.

Figure 4a shows that after structural relaxation, when placed between gold electrodes, the molecules adopt an angle

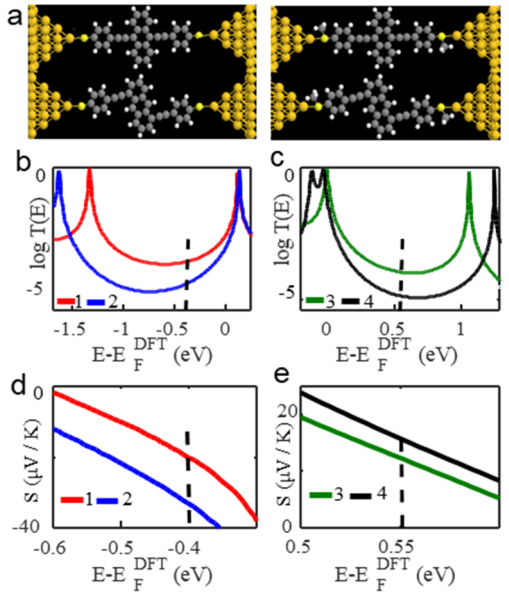

Figure 4. Charge transport in molecular junctions. (a) Schematic illustration of molecular junctions for **1**, **2**, **3**, and **4**. (b, c) Transmission functions $T(E)$ for **1** (red solid line), **2** (blue solid line), **3** (green solid line), and **4** (black solid line). (d, e) Plots of the room-temperature Seebeck coefficients of **1**−**4** as a function of the Fermi energy E_F.

corresponding to the measured tilt angle of the SAM (for different views see Figure S27). It has recently been demonstrated, by comparing $T(E)$ for a single molecule against SAMs consisting of seven molecules,[51] that the $T(E)$ for a SAM is approximately the same as for the single molecule. Figure 4b shows the computed transmission coefficients for all four junctions, while Figure 4d,e shows the corresponding Seebeck coefficients as a function of the Fermi energy E_F. In agreement with previous studies,[27] we find that the closest agreement between theory and experiment is obtained for a Fermi energy near the midgap, indicated by the vertical dashed lines in Figure 4b,c. The computed ratio of their transmission coefficients in gold−molecule−gold junctions (SI, Figure S28) for molecules **1** and **2** (similarly for **3** and **4**) at $E = E_F^{gold}$ is approximately 16. As described above, both molecules exhibit CQI near their gap centers, and the conductance ratio arises from the different degrees of CQI associated with their different connectivities.[36,37,52−57]

Table 1. Experimental Measurements, Standard Uncertainty (std), and Theoretical Calculations for Conductance Ratios (G/G_0) and Seebeck Coefficient (S)[a]

	G/G_0			S (μV/K)		
molecule	expt	std	theor	expt	std	theor
1	7.01×10^{-5}	9×10^{-6}	1.66×10^{-4}	−23.4	4.6	−20.0
2	6.88×10^{-6}	1×10^{-6}	1.05×10^{-5}	−31.8	6.1	−33.0
3	1.28×10^{-4}	5×10^{-6}	1.59×10^{-4}	+12.1	3.0	+12.5
4	9.0×10^{-6}	3×10^{-6}	1.00×10^{-5}	+10.4	1.1	+16.3

[a] $E_F - E_F^{DFT} = -0.4$ eV for **1** and **2**, $E_F - E_F^{DFT} = +0.55$ eV for **3** and **4**; average values are plotted as yellow lines in SI Figure S28.

https://dx.doi.org/10.1021/jacs.9b13578
J. Am. Chem. Soc. 2020, 142, 8555−8560

When the terminal groups of molecules are changed from thioethers to thioacetates, the transmission coefficients for molecules **3** and **4** show the same trend as those associated with molecules **1** and **2** (see Table 1). The change in sign of the thermopower between terminal groups is due to the position of the frontier orbital energies relative to the Fermi energy of gold (Figure 4); for the thioether-terminated molecules (**1** and **2**) the Fermi energy lies close to the LUMO, giving a positive slope and a negative Seebeck coefficient, whereas for the thiolate- (from thioacetate) terminated molecules (**3** and **4**) the HOMO is closer to the Fermi energy, giving a negative slope and a positive Seebeck coefficient.

In summary, through the rational design, synthesis, and implementation of a new family of molecules, we have demonstrated that unequivocal signatures of single-molecule room-temperature CQI, contained in the connectivity-dependent conductance ratio of **1** and **2** (**3** and **4**), can be translated into self-assembled molecular films. In contrast to previous work contrasting DQI with CQI effects in the Seebeck coefficient of a single molecule,[14] here we have examined how different degrees of CQI can be used to control the thermopower of SAMs. Utilizing CQI to control thermoelectricity is useful, since CQI allows the desirable possibility of high conductance, whereas DQI always leads to low conductance. With two different connectivities to the anthracene core, CQI effects lead to measured conductance ratios of $(G_1/G_2)_{exp}$ = 10.2 and $(G_3/G_4)_{exp}$ = 14.3 for SAMs formed from **1** compared to **2** and from **3** compared to **4**), which are comparable with the "magic ratio" of 16 and the single-molecule DFT values of $(G_1/G_2)_{theor}$ = 15.8 and $(G_3/G_4)_{theor}$ = 16.0. Furthermore, we show that the thermoelectrical performance of anthracene-based molecular films can be boosted by a judicious choice of connectivity to electrodes, combined with an optimal choice of terminal groups. Although the effect of CQI on the electrical conductance of SAMs was reported only recently,[58] the above demonstration of CQI-controlled molecular films is the first report of CQI-boosted thermoelectricity. It opens the way to new design strategies for functional ultra-thin-film thermoelectric materials and electronic building blocks for future integrated circuits.

■ ASSOCIATED CONTENT

Supporting Information

The Supporting Information is available free of charge at https://pubs.acs.org/doi/10.1021/jacs.9b13578.

Experimental details including information about the synthesis of the molecules, device fabrication, and characterization; theoretical demonstration of molecular orbitals as well as the calculated transmission coefficient of gold/molecule/gold systems for all molecules (PDF)

■ AUTHOR INFORMATION

Corresponding Authors

Benjamin J. Robinson − *Physics Department, Lancaster University, Lancaster LA1 4YB, U.K.;* orcid.org/0000-0001-8676-6469; Email: b.j.robinson@lancaster.ac.uk

Nicholas J. Long − *Department of Chemistry, Imperial College London, MSRH, White City, London W12 0BZ, U.K.;* orcid.org/0000-0002-8298-938X; Email: n.long@imperial.ac.uk

Lesley F. Cohen − *The Blackett Laboratory, Imperial College London, London SW7 2AZ, U.K.;* Email: l.cohen@imperial.ac.uk

Colin J. Lambert − *Physics Department, Lancaster University, Lancaster LA1 4YB, U.K.;* orcid.org/0000-0003-2332-9610; Email: c.lambert@lancaster.ac.uk

Authors

Xintai Wang − *Physics Department, Lancaster University, Lancaster LA1 4YB, U.K.; The Blackett Laboratory, Imperial College London, London SW7 2AZ, U.K.*

Troy L. R. Bennett − *Department of Chemistry, Imperial College London, MSRH, White City, London W12 0BZ, U.K.*

Ali Ismael − *Physics Department, Lancaster University, Lancaster LA1 4YB, U.K.; Department of Physics, College of Education for Pure Science, Tikrit University, Tikrit, Iraq*

Luke A. Wilkinson − *Department of Chemistry, Imperial College London, MSRH, White City, London W12 0BZ, U.K.;* orcid.org/0000-0002-8550-3226

Joseph Hamill − *Department of Chemistry, Birmingham University, Edgbaston, Birmingham B15 2TT, U.K.*

Andrew J. P. White − *Department of Chemistry, Imperial College London, MSRH, White City, London W12 0BZ, U.K.*

Iain M. Grace − *Physics Department, Lancaster University, Lancaster LA1 4YB, U.K.*

Oleg V. Kolosov − *Physics Department, Lancaster University, Lancaster LA1 4YB, U.K.;* orcid.org/0000-0003-3278-9643

Tim Albrecht − *Department of Chemistry, Birmingham University, Edgbaston, Birmingham B15 2TT, U.K.;* orcid.org/0000-0001-6085-3206

Complete contact information is available at: https://pubs.acs.org/10.1021/jacs.9b13578

Author Contributions

#X.W., T.L.R.B., and A.I. contributed equally.

Notes

The authors declare no competing financial interest.

■ ACKNOWLEDGMENTS

Support from the UK EPSRC is acknowledged, through grant nos. EP/N017188/1, EP/M014452/1, EP/P027156/1, and EP/N03337X/1. Support from the European Commission is provided by the FET Open project 767187 - QuIET. A.I. is grateful for financial assistance from Tikrit University, Iraq, and the Iraqi Ministry of Higher Education (SL-20). N.J.L. is grateful for a Royal Society Wolfson Research Merit Award. L.F.C. and X.W. acknowledge FSRF funding.

■ REFERENCES

(1) Aradhya, S. V.; Venkataraman, L. Single-molecule junctions beyond electronic transport. *Nat. Nanotechnol.* **2013**, *8* (6), 399−410.

(2) Lambert, C. Basic concepts of quantum interference and electron transport in single-molecule electronics. *Chem. Soc. Rev.* **2015**, *44* (4), 875−888.

(3) Xiang, D.; Wang, X.; Jia, C.; Lee, T.; Guo, X. Molecular-scale electronics: from concept to function. *Chem. Rev.* **2016**, *116* (7), 4318−4440.

(4) Jia, C.; Migliore, A.; Xin, N.; Huang, S.; Wang, J.; Yang, Q.; Wang, S.; Chen, H.; Wang, D.; Feng, B.; et al. Covalently bonded single-molecule junctions with stable and reversible photoswitched conductivity. *Science* **2016**, *352* (6292), 1443−1445.

(5) Papadopoulos, T.; Grace, I.; Lambert, C. Control of electron transport through Fano resonances in molecular wires. *Phys. Rev. B: Condens. Matter Mater. Phys.* **2006**, *74* (19), 193306.
(6) Markussen, T.; Schiotz, J.; Thygesen, K. S. Electrochemical control of quantum interference in anthraquinone-based molecular switches. *J. Chem. Phys.* **2010**, *132* (22), 224104.
(7) Vazquez, H.; Skouta, R.; Schneebeli, S.; Kamenetska, M.; Breslow, R.; Venkataraman, L.; Hybertsen, M. Probing the conductance superposition law in single-molecule circuits with parallel paths. *Nat. Nanotechnol.* **2012**, *7* (10), 663−667.
(8) Ballmann, S.; Hartle, R.; Coto, P. B.; Elbing, M.; Mayor, M.; Bryce, M. R.; Thoss, M.; Weber, H. B. Experimental evidence for quantum interference and vibrationally induced decoherence in single-molecule junctions. *Phys. Rev. Lett.* **2012**, *109* (5), 056801.
(9) Aradhya, S. V.; Meisner, J. S.; Krikorian, M.; Ahn, S.; Parameswaran, R.; Steigerwald, M. L.; Nuckolls, C.; Venkataraman, L. Dissecting contact mechanics from quantum interference in single-molecule junctions of stilbene derivatives. *Nano Lett.* **2012**, *12* (3), 1643−1647.
(10) Kaliginedi, V.; Moreno-Garcia, P.; Valkenier, H.; Hong, W.; Garcia-Suarez, V. M.; Buiter, P.; Otten, J. L.; Hummelen, J. C.; Lambert, C. J.; Wandlowski, T. Correlations between molecular structure and single-junction conductance: a case study with oligo(phenylene-ethynylene)-type wires. *J. Am. Chem. Soc.* **2012**, *134* (11), 5262−5275.
(11) Arroyo, C. R.; Tarkuc, S.; Frisenda, R.; Seldenthuis, J. S.; Woerde, C. H.; Eelkema, R.; Grozema, F. C.; van der Zant, H. S. Signatures of quantum interference effects on charge transport through a single benzene ring. *Angew. Chem.* **2013**, *125* (11), 3234−3237.
(12) Ke, S.-H.; Yang, W.; Baranger, H. U. Quantum-interference-controlled molecular electronics. *Nano Lett.* **2008**, *8* (10), 3257−3261.
(13) Guédon, C. M.; Valkenier, H.; Markussen, T.; Thygesen, K. S.; Hummelen, J. C.; Van Der Molen, S. J. Observation of quantum interference in molecular charge transport. *Nat. Nanotechnol.* **2012**, *7* (5), 305−309.
(14) Miao, R.; Xu, H.; Skripnik, M.; Cui, L.; Wang, K.; Pedersen, K. G. L.; Leijnse, M.; Pauly, F.; Wärnmark, K.; Meyhofer, E.; Reddy, P.; Linke, H. Influence of Quantum Interference on the Thermoelectric Properties of Molecular Junctions. *Nano Lett.* **2018**, *18* (9), 5666−5672.
(15) Jia, C.; Famili, M.; Carlotti, M.; Liu, Y.; Wang, P.; Grace, I. M.; Feng, Z.; Wang, Y.; Zhao, Z.; Ding, M.; Xu, X.; Wang, C.; Lee, S.-J.; Huang, Y.; Chiechi, R. C.; Lambert, C. J.; Duan, X. Quantum interference mediated vertical molecular tunneling transistors. *Science Advances* **2018**, *4* (10), No. eaat8237.
(16) Fracasso, D.; Valkenier, H.; Hummelen, J. C.; Solomon, G. C.; Chiechi, R. C. Evidence for Quantum Interference in SAMs of Arylethynylene Thiolates in Tunneling Junctions with Eutectic Ga−In (EGaIn) Top-Contacts. *J. Am. Chem. Soc.* **2011**, *133* (24), 9556−9563.
(17) Carlotti, M.; Kovalchuk, A.; Wächter, T.; Qiu, X.; Zharnikov, M.; Chiechi, R. C. Conformation-driven quantum interference effects mediated by through-space conjugation in self-assembled monolayers. *Nat. Commun.* **2016**, *7* (1), 13904.
(18) Zhang, Y.; Ye, G.; Soni, S.; Qiu, X.; Krijger, T. L.; Jonkman, H. T.; Carlotti, M.; Sauter, E.; Zharnikov, M.; Chiechi, R. C. Controlling destructive quantum interference in tunneling junctions comprising self-assembled monolayers via bond topology and functional groups. *Chemical Science* **2018**, *9* (19), 4414−4423.
(19) Carlotti, M.; Soni, S.; Kumar, S.; Ai, Y.; Sauter, E.; Zharnikov, M.; Chiechi, R. C. Two-Terminal Molecular Memory through Reversible Switching of Quantum Interference Features in Tunneling Junctions. *Angew. Chem., Int. Ed.* **2018**, *57* (48), 15681−15685.
(20) Carlotti, M.; Soni, S.; Qiu, X.; Sauter, E.; Zharnikov, M.; Chiechi, R. C. Systematic experimental study of quantum interference effects in anthraquinoid molecular wires. *Nanoscale Advances* **2019**, *1* (5), 2018−2028.
(21) Rincón-García, L.; Evangeli, C.; Rubio-Bollinger, G.; Agraït, N. Thermopower measurements in molecular junctions. *Chem. Soc. Rev.* **2016**, *45* (15), 4285−4306.
(22) Rincón-García, L.; Ismael, A. K.; Evangeli, C.; Grace, I.; Rubio-Bollinger, G.; Porfyrakis, K.; Agraït, N.; Lambert, C. J. Molecular design and control of fullerene-based bi-thermoelectric materials. *Nat. Mater.* **2016**, *15*, 289.
(23) Al-Khaykanee, M. K.; Ismael, A. K.; Grace, I.; Lambert, C. J. Oscillating Seebeck coefficients in π-stacked molecular junctions. *RSC Adv.* **2018**, *8* (44), 24711−24715.
(24) Ismael, A. K.; Grace, I.; Lambert, C. J. Increasing the thermopower of crown-ether-bridged anthraquinones. *Nanoscale* **2015**, *7* (41), 17338−17342.
(25) Cui, L.; Miao, R.; Jiang, C.; Meyhofer, E.; Reddy, P. Perspective: Thermal and thermoelectric transport in molecular junctions. *J. Chem. Phys.* **2017**, *146* (9), 092201.
(26) Yzambart, G.; Rincón-García, L.; Al-Jobory, A. A.; Ismael, A. K.; Rubio-Bollinger, G.; Lambert, C. J.; Agraït, N.; Bryce, M. R. Thermoelectric Properties of 2,7-Dipyridylfluorene Derivatives in Single-Molecule Junctions. *J. Phys. Chem. C* **2018**, *122* (48), 27198−27204.
(27) Geng, Y.; Sangtarash, S.; Huang, C.; Sadeghi, H.; Fu, Y.; Hong, W.; Wandlowski, T.; Decurtins, S.; Lambert, C. J.; Liu, S. X. Magic ratios for connectivity-driven electrical conductance of graphene-like molecules. *J. Am. Chem. Soc.* **2015**, *137* (13), 4469−4476.
(28) Sangtarash, S.; Huang, C.; Sadeghi, H.; Sorohhov, G.; Hauser, J.; Wandlowski, T.; Hong, W.; Decurtins, S.; Liu, S. X.; Lambert, C. J. Searching the Hearts of Graphene-like Molecules for Simplicity, Sensitivity, and Logic. *J. Am. Chem. Soc.* **2015**, *137* (35), 11425−11431.
(29) Lambert, C. J.; Liu, S. X. A Magic Ratio Rule for Beginners: A Chemist's Guide to Quantum Interference in Molecules. *Chem. - Eur. J.* **2018**, *24* (17), 4193−4201.
(30) Jia, C.; Guo, X. Molecule-electrode interfaces in molecular electronic devices. *Chem. Soc. Rev.* **2013**, *42* (13), 5642−5660.
(31) Hong, W.; Manrique, D. Z.; Moreno-Garcia, P.; Gulcur, M.; Mishchenko, A.; Lambert, C. J.; Bryce, M. R.; Wandlowski, T. Single molecular conductance of tolanes: experimental and theoretical study on the junction evolution dependent on the anchoring group. *J. Am. Chem. Soc.* **2012**, *134* (4), 2292−2304.
(32) Weidner, T.; Ballav, N.; Siemeling, U.; Troegel, D.; Walter, T.; Tacke, R.; Castner, D. G.; Zharnikov, M. Tripodal Binding Units for Self-Assembled Monolayers on Gold: A Comparison of Thiol and Thioether Headgroups. *J. Phys. Chem. C* **2009**, *113* (45), 19609−19617.
(33) Piotrowski, P.; Pawłowska, J.; Pawłowski, J.; Czerwonka, A. M.; Bilewicz, R.; Kaim, A. Self-assembly of thioether functionalized fullerenes on gold and their activity in electropolymerization of styrene. *RSC Adv.* **2015**, *5* (105), 86771−86778.
(34) del Carmen Gimenez-Lopez, M.; Räisänen, M. T.; Chamberlain, T. W.; Weber, U.; Lebedeva, M.; Rance, G. A.; Briggs, G. A. D.; Pettifor, D.; Burlakov, V.; Buck, M.; Khlobystov, A. N. Functionalized Fullerenes in Self-Assembled Monolayers. *Langmuir* **2011**, *27* (17), 10977−10985.
(35) Ulčakar, L.; Rejec, T.; Kokalj, J.; Sangtarash, S.; Sadeghi, H.; Ramšak, A.; Jefferson, J. H.; Lambert, C. J. On the resilience of magic number theory for conductance ratios of aromatic molecules. *Sci. Rep.* **2019**, *9* (1), 3478.
(36) Tsuji, Y.; Staykov, A.; Yoshizawa, K. Orbital views of molecular conductance perturbed by anchor units. *J. Am. Chem. Soc.* **2011**, *133* (15), 5955−5965.
(37) Yoshizawa, K.; Tada, T.; Staykov, A. Orbital views of the electron transport in molecular devices. *J. Am. Chem. Soc.* **2008**, *130* (29), 9406−9413.
(38) Li, X.; Staykov, A.; Yoshizawa, K. Orbital Views of the Electron Transport through Polycyclic Aromatic Hydrocarbons with Different Molecular Sizes and Edge Type Structures. *J. Phys. Chem. C* **2010**, *114* (21), 9997−10003.

https://dx.doi.org/10.1021/jacs.9b13578
J. Am. Chem. Soc. 2020, 142, 8555−8560

(39) Inkpen, M. S.; White, A. J. P.; Albrecht, T.; Long, N. J. Avoiding problem reactions at the ferrocenyl-alkyne motif: a convenient synthesis of model, redox-active complexes for molecular electronics. *Dalton Transactions* **2014**, *43* (41), 15287−15290.
(40) Garcia, R.; Martinez, R. V.; Martinez, J. Nano-chemistry and scanning probe nanolithographies. *Chem. Soc. Rev.* **2006**, *35* (1), 29−38.
(41) Amro, N. A.; Xu, S.; Liu, G. Y. Patterning surfaces using tip-directed displacement and self-assembly. *Langmuir* **2000**, *16* (7), 3006−3009.
(42) Kaholek, M.; Lee, W. K.; LaMattina, B.; Caster, K. C.; Zauscher, S. Fabrication of stimulus-responsive nanopatterned polymer brushes by scanning-probe lithography. *Nano Lett.* **2004**, *4* (2), 373−376.
(43) Orata, D.; Buttry, D. A. Determination of Ion Populations and Solvent Content as Functions of Redox State and Ph in Polyaniline. *J. Am. Chem. Soc.* **1987**, *109* (12), 3574−3581.
(44) Sauerbrey, G. Verwendung Von Schwingquarzen Zur Wagung Dunner Schichten Und Zur Mikrowagung. *Eur. Phys. J. A* **1959**, *155* (2), 206−222.
(45) Weiss, E. A.; Kaufman, G. K.; Kriebel, J. K.; Li, Z.; Schalek, R.; Whitesides, G. M. Si/SiO2-Templated formation of ultraflat metal surfaces on glass, polymer, and solder supports: Their use as substrates for self-assembled monolayers. *Langmuir* **2007**, *23* (19), 9686−9694.
(46) Banner, L. T.; Richter, A.; Pinkhassik, E. Pinhole-free large-grained atomically smooth Au(111) substrates prepared by flame-annealed template stripping. *Surf. Interface Anal.* **2009**, *41* (1), 49−55.
(47) Burnham, N. A.; Colton, R. J.; Pollock, H. M. Work-Function Anisotropies as an Origin of Long-Range Surface Forces - Reply. *Phys. Rev. Lett.* **1993**, *70* (2), 247−247.
(48) Weihs, T. P.; Nawaz, Z.; Jarvis, S. P.; Pethica, J. B. Limits of Imaging Resolution for Atomic Force Microscopy of Molecules. *Appl. Phys. Lett.* **1991**, *59* (27), 3536−3538.
(49) Gomar-Nadal, E.; Ramachandran, G. K.; Chen, F.; Burgin, T.; Rovira, C.; Amabilino, D. B.; Lindsay, S. M. Self-assembled monolayers of tetrathiafulvalene derivatives on Au(111): Organization and electrical properties. *J. Phys. Chem. B* **2004**, *108* (22), 7213−7218.
(50) Ferrer, J.; Lambert, C. J.; García-Suárez, V. M.; Manrique, D. Z.; Visontai, D.; Oroszlany, L.; Rodríguez-Ferradás, R.; Grace, I.; Bailey, S.; Gillemot, K.; et al. GOLLUM: a next-generation simulation tool for electron, thermal and spin transport. *New J. Phys.* **2014**, *16* (9), 093029.
(51) Herrer, L.; Ismael, A.; Martín, S.; Milan, D. C.; Serrano, J. L.; Nichols, R. J.; Lambert, C.; Cea, P. Single molecule vs. large area design of molecular electronic devices incorporating an efficient 2-aminepyridine double anchoring group. *Nanoscale* **2019**, *11* (34), 15871−15880.
(52) Coulson, C.; Rushbrooke, G. Note on the method of molecular orbitals. *Mathematical Proceedings of the Cambridge Philosophical Society*; Cambridge University Press: 1940; pp 193−200.
(53) Zhao, X.; Geskin, V.; Stadler, R. Destructive quantum interference in electron transport: A reconciliation of the molecular orbital and the atomic orbital perspective. *J. Chem. Phys.* **2017**, *146* (9), 092308.
(54) Lambert, C. J.; Liu, S. X. A Magic Ratio Rule for Beginners: A Chemist's Guide to Quantum Interference in Molecules. *Chem. - Eur. J.* **2018**, *24* (17), 4193−4201.
(55) Garner, M. H.; Li, H.; Chen, Y.; Su, T. A.; Shangguan, Z.; Paley, D. W.; Liu, T.; Ng, F.; Li, H.; Xiao, S.; Nuckolls, C.; Venkataraman, L.; Solomon, G. C. Comprehensive suppression of single-molecule conductance using destructive σ-interference. *Nature* **2018**, *558* (7710), 415−419.
(56) Naghibi, S.; Ismael, A. K.; Vezzoli, A.; Al-Khaykanee, M. K.; Zheng, X.; Grace, I. M.; Bethell, D.; Higgins, S. J.; Lambert, C. J.; Nichols, R. J. Synthetic Control of Quantum Interference by Regulating Charge on a Single Atom in Heteroaromatic Molecular Junctions. *J. Phys. Chem. Lett.* **2019**, *10* (20), 6419−6424.
(57) Ismael, A. K.; Grace, I.; Lambert, C. J. Connectivity dependence of Fano resonances in single molecules. *Phys. Chem. Chem. Phys.* **2017**, *19* (9), 6416−6421.
(58) Famili, M.; Jia, C.; Liu, X.; Wang, P.; Grace, I. M.; Guo, J.; Liu, Y.; Feng, Z.; Wang, Y.; Zhao, Z.; Decurtins, S.; Häner, R.; Huang, Y.; Liu, S.-X.; Lambert, C. J.; Duan, X. Self-Assembled Molecular-Electronic Films Controlled by Room Temperature Quantum Interference. *Chem.* **2019**, *5* (2), 474−484.

https://dx.doi.org/10.1021/jacs.9b13578
J. Am. Chem. Soc. 2020, 142, 8555−8560